ChemBioChem

Combining Chemistry and Biology

Chemistry Europe

European Chemical Societies Publishing

# Accepted Article

**Title:** Biosynthesis of the Fungal Organophosphonate Fosfonochlorin Involves an Iron(II) and 2-(Oxo)glutarate Dependent Oxacyclase

**Authors:** Simanga R. Gama, Toda Stankovic, Kendall Hupp, Ahmed Al Hejami, Mimi McClean, Alysa Evans, Diane Beauchemin, Friedrich Hammerschmidt, Katharina Pallitsch, and David L. Zechel



**To be cited as:** *ChemBioChem* 10.1002/cbic.202100352

**Link to VoR:** https://doi.org/10.1002/cbic.202100352

WILEY-VCH

10.1002/cbic.202100352

WILEY-VCH

FULL PAPER

# Biosynthesis of the Fungal Organophosphonate Fosfonochlorin Involves an Iron(II) and 2-(Oxo)glutarate Dependent Oxacyclase

Simanga R. Gama[a], Toda Stankovic[b], Kendall Hupp[a], Ahmed Al Hejami[a], Mimi McClean[a], Alysa Evans[a], Diane Beauchemin[a], Friedrich Hammerschmidt[b], Katharina Pallitsch*[b], David L. Zechel*[a]

[a] Dr. Simanga R. Gama, Kendall Hupp, Dr. Ahmed Al Hejami, Mimi McClean, Alysa Evans, Prof. Dr. Diane Beauchemin, Prof. Dr. David L. Zechel
Department of Chemistry
Queen's University
Kingston, Ontario, Canada, K7L 3N6
E-mail: dlzechel@chem.queensu.ca

[b] Toda Stankovic, Prof. Dr. Friedrich Hammerschmidt, Dr. Katharina Pallitsch
Institut für Organische Chemie
Universität Wien
A-1090, Wien, Österreich
E-mail: katharina.pallitsch@univie.ac.at

Supporting information for this article is given via a link at the end of the document.

The fungal metabolite Fosfonochlorin features a chloroacetyl moiety that is unusual within known phosphonate natural product biochemistry. Putative biosynthetic genes encoding Fosfonochlorin in *Fusarium* and *Talaromyces* spp. were investigated through reactions of encoded enzymes with synthetic substrates and isotope labelling studies. We show that early biosynthetic steps for Fosfonochlorin involves the reduction of phosphonoacetaldehyde to form 2-hydroxyethylphosphonic acid, followed by oxidative intramolecular cyclization of the resulting alcohol to form (*S*)-epoxyethylphosphonic acid. The latter reaction is catalyzed by FfnD, a rare example of a non-heme iron / 2-(oxo)glutarate dependent oxacyclase. In contrast, FfnD behaves as a more typical oxygenase with ethylphosphonic acid, producing (*S*)-1-hydroxyethylphosphonic acid. FfnD thus represents a new example of a ferryl generating enzyme that can suppress the typical oxygen rebound reaction that follows abstraction of a substrate hydrogen by a ferryl oxygen, thereby directing the substrate radical towards a fate other than hydroxylation.

## Introduction

Fosfonochlorin **1** belongs to the steadily growing and structurally diverse class of organophosphonate (Pn) natural products (**Scheme 1A**) whose distinguishing chemical feature is a hydrolytically and thermally stable carbon-phosphorus (C-P) bond.[1] Familiar examples of natural product Pns include the cell membrane constituent 2-aminoethylphosphonic acid **2** (or Ciliatine) and the antibiotic Fosfomycin **3**, which is one of many commercially used Pn.[1,2] Pns were for a long time believed to be of low environmental importance due to the limited knowledge about their structures, occurrence, and pathways involved in their metabolism. This perspective has undergone a paradigm shift, largely driven by genomics, with the discovery that Pn biosynthesis[3-7] and catabolism[8-11] occurs widely in the microbial world. A survey in 2012 revealed the presence of Pn biosynthetic and catabolic genes in ~10% and 40%, respectively, of published microbial genomes.[12] Microbial Pn metabolism can even influence global P and C cycles, most dramatically seen in microbial biosynthesis and catabolism of the simplest Pn, methylphosphonic acid, which leads to supersaturating levels of methane in ocean surface waters.[13,14] In this light Pns are unique amongst natural products, not only serving as a life limiting nutrient for microbes that live in phosphate depleted environments,[15] but also as useful source of bioactive compounds. The enzymology encoded by Pn metabolic gene clusters remains underexplored, and what has been characterized has often proven to be mechanistically unusual.[16]

**1** stands out as a rare example of a halogenated Pn, with phosphoiodyn A **4** being the only other known example.[17] **1** was first isolated from fungi within the genera *Fusarium* and *Talaromyces* on the basis of its antibacterial spheroplast forming activity[18] but its biosynthetic origin remains unknown. The identification of microbial biosynthetic gene clusters (BGCs) encoding Pn biosynthesis is facilitated by the distinct C-P bond forming enzymatic step. Nearly all known Pn biosynthetic pathways form C-P bonds through the isomerization of

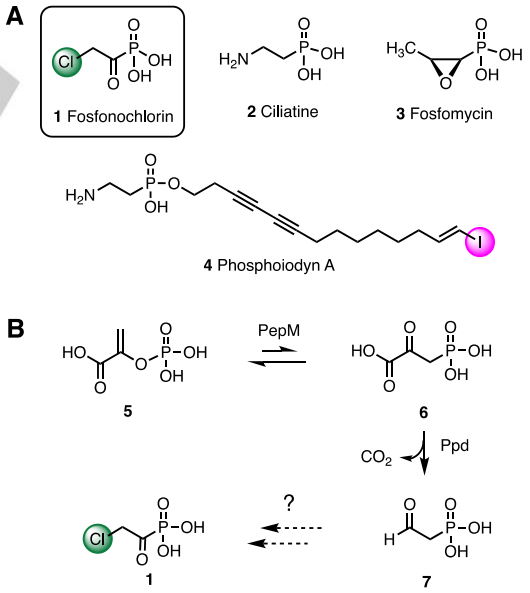


**Scheme 1.** (A) Examples of organophosphonate natural products. (B) Initial steps in the biosynthesis of **1**.

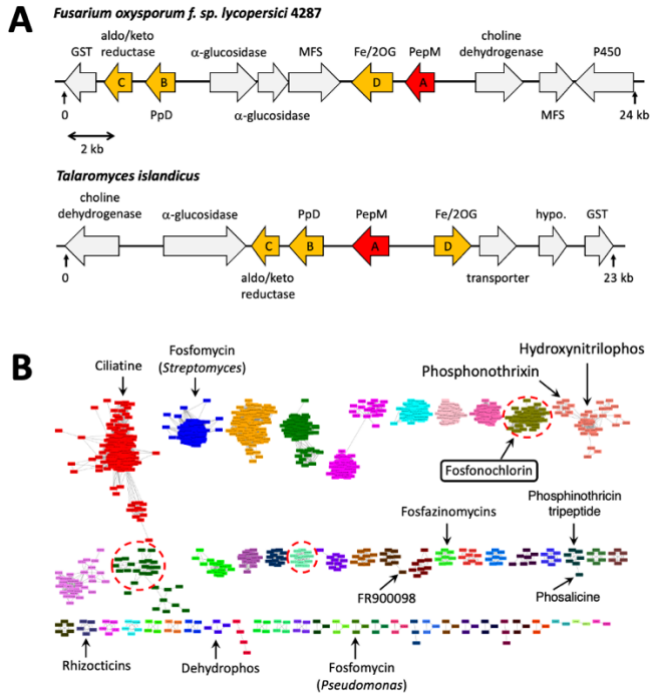


**Figure 1.** Identification of conserved biosynthetic genes encoding **1**. (**A**) Representative genome loci with core biosynthetic genes proposed to encode **1** highlighted (accession numbers: NC_030993.1 and CVMT01000003.1). (**B**) Sequence similarity network based on PepM sequences. Clusters that contain PepM from *Fusarium* and *Talaromyces* fungal species are highlighted with dashed circles, with the proposed cluster for **1** shown. Clusters containing PepM sequences from known biosynthetic pathways are labelled with the corresponding Pn products.

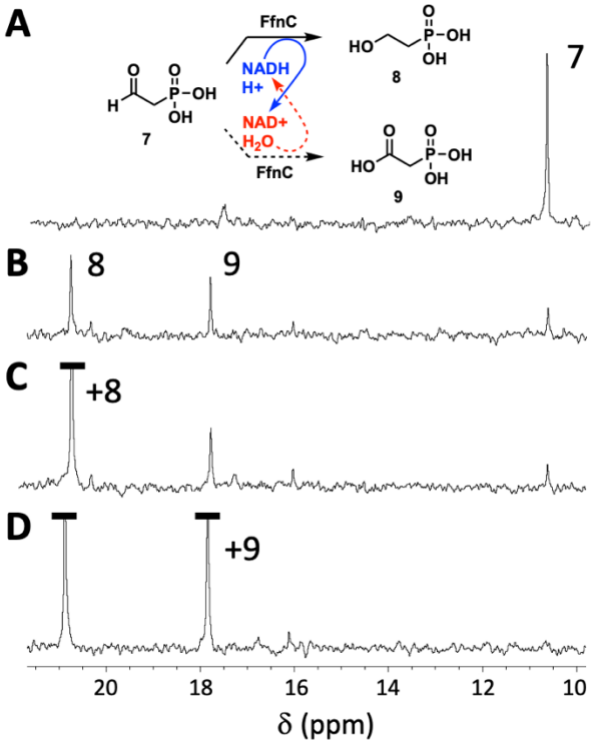


**Figure 2.** {$^1$H} $^{31}$P-NMR spectral analysis of the FfnC reaction with **7** and NADH. (**A**) Spectrum for **7** (δ = 10.6 ppm) in the presence of all reaction components other than enzyme. (**B**) Reaction of FfnC with **7** and NADH (1 mM each) for 16 hrs, 25°C, pH 7. (**C, D**) Addition of authentic **8** (δ = 20.6 ppm) and **9** (δ = 17.7 ppm) to the NMR sample. Signals are truncated for clarity.

phosphoenolpyruvate **5** to phosphonopyruvate **6** by phosphoenolpyruvate phosphomutase (PepM) (**Scheme 1B**),[1] which makes *pepM* a useful marker for identifying BGCs encoding Pns.[3,5,6,19] Formation of **6** is thermodynamically unfavorable and is therefore typically followed by a 'trapping' reaction, such as decarboxylation by the thiamine dependent enzyme phosphonopyruvate decarboxylase (Ppd) to form phosphonoacetaldehyde **7**.[1] However, the steps necessary to transform the acetaldehyde moiety of **7** to the chloroacetyl moiety of **1** are without precedence in known Pn biochemistry.[1] In this paper we characterize the functions of enzymes involved in the early steps of **1** biosynthesis, including a rare example of an oxacyclization reaction catalyzed by a non-heme iron / 2-(oxo)glutarate dependent (Fe/2OG) dioxygenase.

## Results and Discussion

### Conserved genes encoding Fosfonochlorin biosynthesis

A *pepM* sequence led Vinas and coworkers to identify a putative biosynthetic gene cluster encoding **1** in the genome of *F. oxysporum f* sp. *lycopersici* 4287.[20] Within this cluster the gene encoding PepM (herein denoted FfnA) is flanked by genes predicted to encode Ppd (FfnB), an aldo/keto reductase (FfnC), and a Fe/2OG dioxygenase (FfnD). A homologous set of genes is observed in *Talaromyces islandicus* (**Figure 1A**). To examine the conservation of these genes in the greater context of Pn biosynthetic gene clusters we constructed a sequence similarity network (SSN) based on PepM sequences using the EFI-EST tool (**Figure 1B**).[21] The degree of similarity between PepM sequences has been previously shown to correlate with the *pepM* gene neighbourhood similarity, and by extension is reflective of Pn structural diversity and biosynthetic origins.[5] In the PepM SSN, sequences could be resolved into clusters that correspond to known biosynthetic pathways, including that of **2**, **3**, phosphonothrixin, hydroxynitrilaphos, rhizocticins, dehydrophos, FR90098, fosfazinomycins, phosphinothricin, and phosalicine.[6,22] The FfnA sequence appears in a distinct cluster that is represented by 35 strains of *Fusarium* sp. and one strain of *Talaromyces* that share the genes encoding FfnABCD. On this basis we hypothesized that *ffnABCD* encodes a conserved set of reactions leading to **1**.

### Phosphonoacetaldehyde reductase FfnC

We hypothesized that FfnC catalyzes the reduction of **7** to form 2-hydroxyethylphosphonic acid **8** (**Figure 2**), which is a key intermediate in several Pn biosynthetic pathways,[1] including methylphosphonic acid, **3**, dehydrophos, and glufosinate.[13,23] FfnC shows weak sequence identity (13-14%) with the group III metal ion dependent alcohol dehydrogenases FomC, DhpG, and PhpC that were previously shown to reduce **7** to **8** using NAD(P)H.[23,24] However, greater identity is observed with members of the AKR7A subfamily of metal ion independent aldo/keto reductases, where FfnC shares 43-46% sequence identity with the structurally characterized aflatoxin B1 aldehyde reductases from rat, mouse, and human (**Figure S1**). All of the residues involved in NADH binding are conserved, as well as

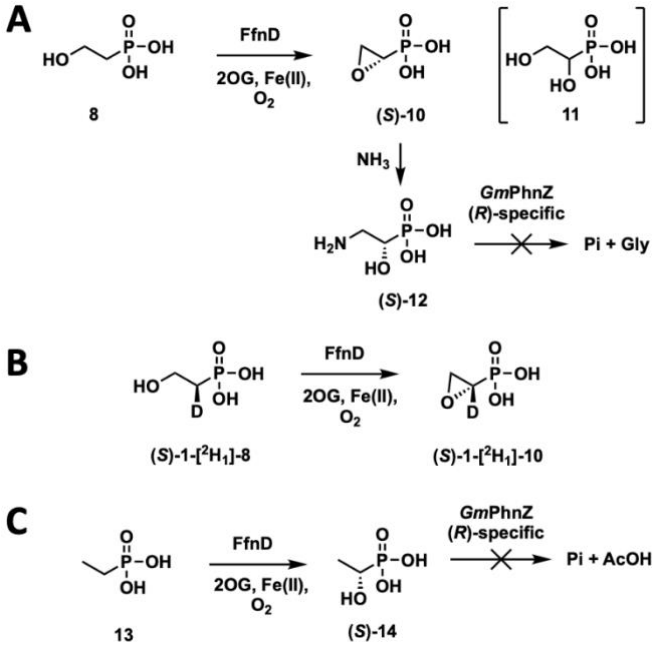


**Scheme 2.** Reactions and stereospecificity of FfnD.

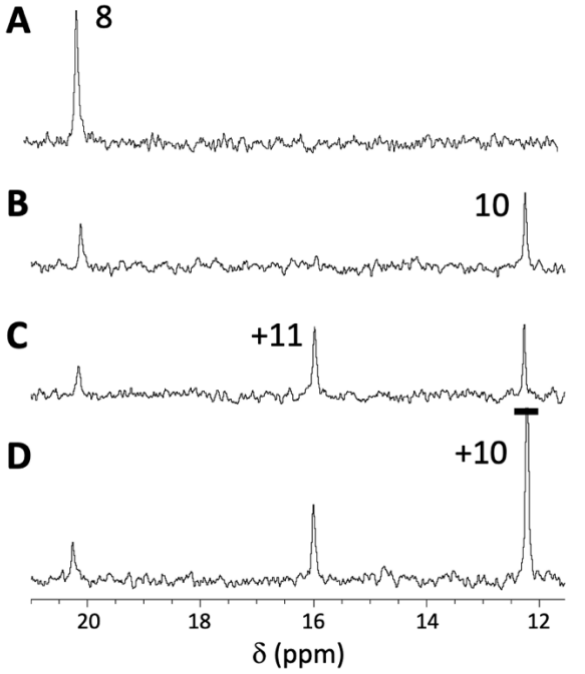


**Figure 3.** {$^{1}$H} $^{31}$P-NMR spectral analysis of the reaction of FfnD with **8**. (A) Spectrum for **8** (δ = 20.3 ppm) in the presence of all reaction components other than enzyme. (B) Reaction of FfnD with **8**. (C, D) Addition of synthetic **11** (δ = 16.1 ppm) and **10** (δ = 12.3 ppm) to the NMR sample. The signal for **10** in (D) is truncated for clarity.

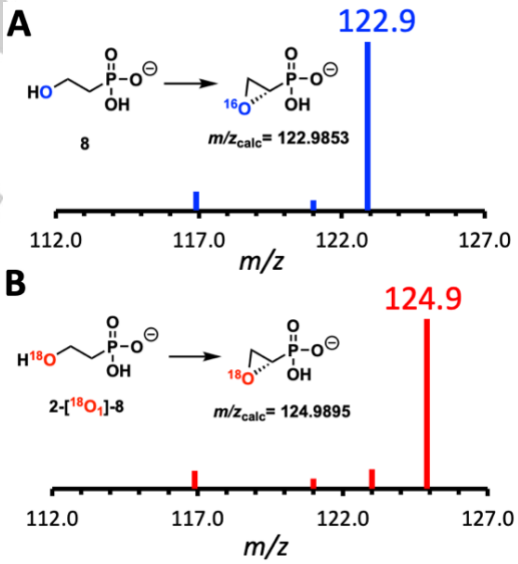


**Figure 4.** UPLC-ESI-MS analysis (negative mode) of the FfnD reaction product **10** formed from (A) **8** and (B) 2-[$^{18}O_1$]-**8**. Formation of **10** was confirmed by $^{31}$P-NMR prior to analysis.

many of the predicted residues involved in substrate binding and catalysis.[25,26] To examine the function of FfnC (XP_018236324.1), the codon optimized gene encoding an *N*-terminal $His_6$ tag was expressed in *E. coli* and the corresponding enzyme and was purified by Ni-NTA chromatography (**Figure S2A**). Purified FfnC was reacted with **7** (1 mM) and a stoichiometric amount of NADH over 16 hrs at 25°C. As followed by $^{31}$P-NMR spectroscopy, **7** (δ = 10.6 ppm) was converted by FfnC to **8** (δ = 20.3 ppm) and, surprisingly, phosphonoacetate **9** (δ = 17.4 ppm) (**Figure 2A and B**). Both products **8** and **9** were confirmed by addition of a synthetic standards to the NMR sample (**Figure 2C and D**). **9** is presumably the result of the oxidation of **7** by FfnC utilizing the NAD+ that is formed during the reducing reaction. Accordingly, **7** is cleanly converted to **8** when an excess of NADH (5-fold) is used with FfnC (**Figure S3**). This indicates that NADH and NAD+ can compete for the active site of FfnC, and lead to competing oxidizing and reducing reactions. The oxidation reaction is notable as FfnC lacks the conserved nucleophilic Cys residue that is used by aldehyde dehydrogenases to form a covalent thiohemiacetal intermediate, such as the phosphonoacetaldehyde oxidase PhnY, which specifically oxidizes **7** to **9**.[27]

## FfnD is a Fe/2OG dependent oxacyclase

We then examined the function of the predicted Fe/2OG dioxygenase FfnD (XP_018236329.1). FfnD shares weak sequence identity (18-24%) to phosphonate biosynthetic Fe/2OG dioxygenases FrbJ (FR-900098 biosynthesis)[28] and DhpA (dehydrophos biosynthesis),[29] including the predicted active site residues involved in Fe(II) and 2OG binding (**Figure S4**). The Fe/2OG oxygenase DhpA has been shown to perform α-hydroxylation of **8** to form 1,2-dihydroxyethylphosphonic acid **11**, therefore we hypothesized FfnD would perform a similar reaction (**Scheme 2A**). The codon optimized gene encoding FfnD was expressed in *E. coli* and the resulting $His_6$ tagged enzyme purified by Ni-NTA chromatography (**Figure S2B**). ICP-OES analysis indicated that purified FfnD contained 8.1 ± 0.2% Fe (n = 3) on a molar basis and thus was predominantly in apo-form. Incubation of FfnD with **8** in the presence of 2OG and ferrous iron led to the formation of **10** with a $^{31}$P-NMR signal at δ = 12.3 ppm (**Figure 3A** and **B**). The reaction could be driven to completion and no other significant products were observed by $^{31}$P-NMR spectroscopy (**Figure S6A**), indicating that **10** is unlikely to be off-pathway product. The signal for **10** did not correspond to the anticipated α-hydroxylation product **11** (δ = 16.1 ppm, **Figure 3C**). Instead, the chemical shift value for **10** is similar to that reported for epoxyphosphonic acids[30] such as Fosfomycin (δ = 11.9 ppm).[31]

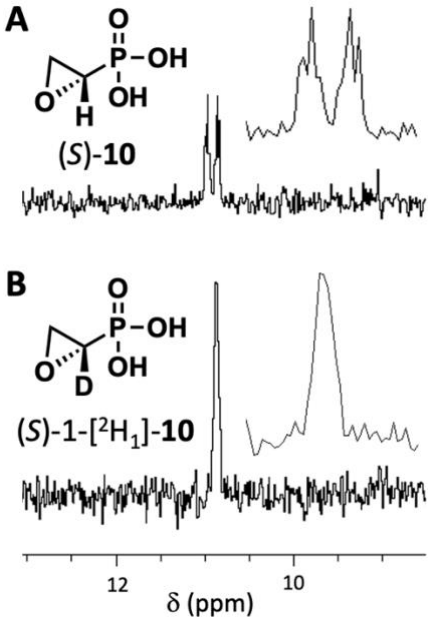


**Figure 5.** $^{1}H$-$^{31}P$ coupled NMR spectra of **10** produced by FfnD from (A) **8** and (B) (*S*)-1-[$^{2}H_1$]-**8**. Insets show expansions of signals.

This was confirmed by addition of synthetic epoxyethylphosphonic acid **10** to the NMR sample (**Figure 3D**). High resolution mass spectrometric analysis of the FfnD reaction mixture also revealed a molecular ion *m/z* = 122.9856 ([M-H]-) that corresponds to the calculated value for **10** ($m/z_{calc}$ = 122.9853) (**Figure S5**). Reaction of FfnD with 2-[$^{18}$O]-**8** produced $^{18}$O labelled **10** as the major product as shown by MS (**Figure 4**), indicating that the 2-hydroxyl of **8** is the source of the epoxide oxygen in **10**. Overall, these experiments establish that FfnD is an Fe/2OG dependent oxacyclase that converts **8** to the epoxide **10** through a dehydrogenation reaction.

## Stereochemical analysis of the FfnD oxacyclization reaction

To probe the stereospecificity of the FfnD oxacyclase reaction, the epoxide **10** was reacted with ammonia[32] to form 2-amino-1-hydroxyethylphosphonic acid **12** (**Scheme 2A, Figure S6A and B**). The aminolysis product was confirmed by addition of synthetic **12** to the NMR sample (**Figure S6C**). **12** was unreactive towards the mixed valence diiron oxygenase *Gm*PhnZ1 (**Figure S6D**), which is specific for converting (*R*)-**12** into inorganic phosphate (Pi) and glycine (**Figure S5E**).[33] Therefore, the aminolysis product is (*S*)-**12** and by extension the FfnD epoxide product is (*S*)-**10**. Next, FfnD was reacted with (*S*)-1-[$^{2}H_1$]-**8** (**Scheme 2B**) and the resulting product was analyzed by $^{1}H$-$^{31}P$ coupled NMR spectroscopy. The apparent doublet-of-triplets coupling pattern for (*S*)-**10** (**Figure 5A**) is not observed in the reaction product derived from (*S*)-1-[$^{2}H_1$]-**8** (**Figure 5B**), indicating retention of deuterium at C1 in (*S*)-**10**. Overall, these results show that the pro-*R* hydrogen of **8** is abstracted by FfnD in forming (*S*)-**10**, and that stereochemistry at C1 is retained during oxacyclization with the substrate 2-hydoxyl. To our surprise, no reaction was observed with FfnD and the di-deuterium labelled substrate 1-[$^{2}H_2$]-**8** under the same reaction conditions used with (*S*)-1-[$^{2}H_1$]-**8**. Only with 5-times greater concentration of FfnD was partial conversion (~20%) to (*S*)-**10** observed over 18 hrs (**Figure S7**).

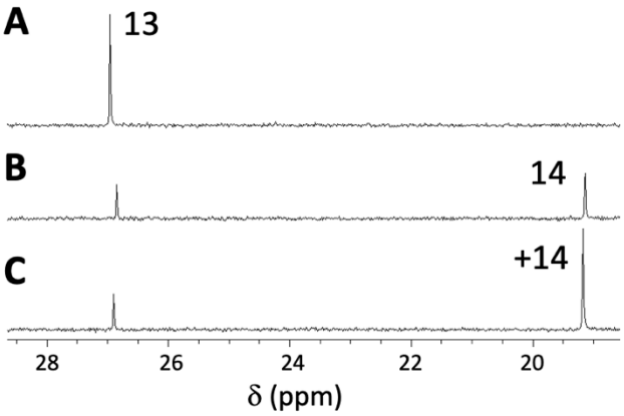


**Figure 6.** {$^{1}H$} $^{31}P$ NMR spectroscopic analysis of the reaction of FfnD with **13**. (A) Spectrum of **13** (δ = 27 ppm). (B) Reaction of FfnD with **13**. (C) Addition of synthetic **14** (δ = 19.2 ppm) to the NMR sample.

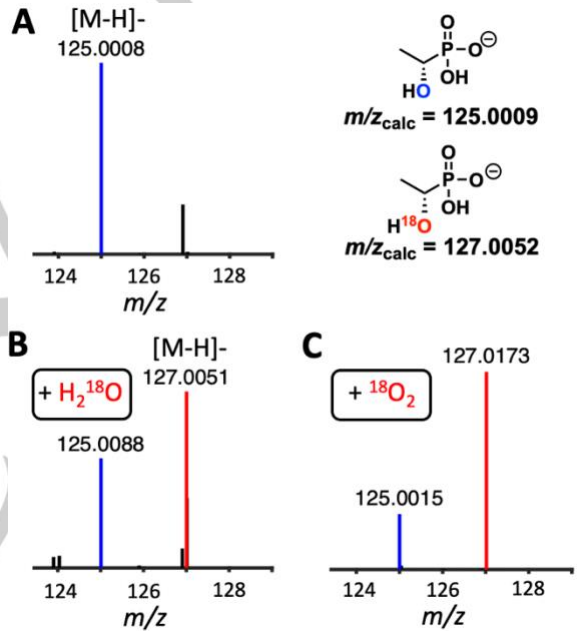


**Figure 7.** (A) HR-ESI-MS analysis the FfnD reaction with **13**. (B) Reaction in the presence of $H_2O^{18}$ (60% v/v). (C) Reaction under an atmosphere of $^{18}O_2$.

This result is indicative of a large primary deuterium kinetic isotope effect arising from rate limiting abstraction of the pro-*R* hydrogen.

## FfnD can also perform hydroxylation

The substrate scope of FfnD was examined with a series of Pns. FfnD was unreactive towards methylphosphonic acid, 2-aminoethylphosphonic acid, phosphonoacetaldehyde, **11**, phosphonoacetate, aminomethylphosphonic acid, glyphosate, 3-amino-1-propenyl phosphonic acid, and ethylenylphosphonic acid. However, reaction of FfnD with ethylphosphonic acid **13** produced 1-hydroxyethylphosphonic acid **14** (**Scheme 2C, Figure 6**) as confirmed by addition of a synthetic standard (**Figure 6C**) and HR-ESI-MS (**Figure 7A**, observed *m/z* = 125.0008, [M-H]-, $m/z_{calc}$ = 125.0009). Therefore, unlike the oxacyclase activity observed with **8**, FfnD functions as a hydroxylase with **13**. The

stereochemistry of α-hydroxylation was probed by reacting FfnD produced **14** with *Gm*PhnZ1, which is specific for conversion of (*R*)-**14** to Pi and acetate.[33] No reaction was observed by $^{31}$P-NMR spectroscopy (**Figure S8**), indicating that FfnD converts **13** to (*S*)-**14**. Therefore, the α-hydroxylation reaction catalyzed by FfnD follows the same stereospecificity as the oxacyclization reaction. The α-hydroxylation reaction of FfnD was also investigated through $^{18}$O labelling experiments. Reaction of FfnD with **13** in the presence of $H_2{}^{18}O$ (~60% v/v) produced $^{18}$O-labelled **14** as shown HR-ESI-MS spectroscopy (**Figure 7B**), as did a reaction under an atmosphere of $^{18}O_2$ (**Figure 7C**). Incorporation of $^{18}$O into **14** via solvent or molecular oxygen is consistent with rapid oxygen atom exchange between a ferryl or Fe(III)-OH intermediate and water.[34-36] While **13** is significant for studying the mechanism of FfnD, it is unlikely to be the native substrate for this enzyme. Unlike **8**, which is a key Pn biosynthetic intermediate in several microbial pathways,[1] **13** is not a known microbial secondary metabolite. However, **13** can form abiotically and has been observed in trace amounts in meteorites.[37]

## FfnD adds to the growing catalytic repertoire of Fe/2OG enzymes

The FfnD reaction is an interesting example in how the fate of a substrate radical intermediate can be controlled upon generation by a ferryl species. The typical outcome arising from abstraction of a substrate hydrogen by a Fe(IV)=O species to form a Fe(III)-OH intermediate is a radical coupling (or 'rebound') of the ferric bound hydroxide with the substrate carbon radical, leading to substrate hydroxylation. The oxacyclization reaction catalyzed by FfnD to form **10** rather than **11** indicates that the rebound step is suppressed in preference for radical coupling between the 2-hydroxyl and C1 of **8**. By contrast, in the absence of a substrate 2-hydroxyl, FfnD catalyzes hydroxylation of **13** to form **14**. A growing number of Fe/2OG enzymes are known to supress rebound and direct the substrate radical intermediate to a different reaction manifold, including cyclization, ring contraction, desaturation, epimerization, endoperoxidation, and halogenation.[38,39] Examples of Fe/2OG dependent oxacyclases include hyoscyamine 6β-hydroxylase (H6H),[34] *N*-acetylnorloline synthase (LolO),[34] clavaminate synthase (CAS),[39] and the orthosomycin-associated oxygenases EvdO1, EvdO2, AviO1, and HygX.[40] A close analog of the FfnD oxacyclization reaction is seen in the formation of the epoxide ring of Fosfomycin **3** by 2-hydroxypropylphosphonic acid epoxidase (HppE). However, HppE differs from FfnD in several critical ways, and thus will likely differ in its oxacyclization mechanism. For example, HppE is 2OG independent and utilizes $H_2O_2$, rather than $O_2$, as an oxidant.[41,42] Additionally, unlike FfnD, HppE promotes inversion of stereochemistry at C1 of the Pn substrate during ring closure.[43] A major question is how the ferryl species formed by these enzymes interacts with their respective substrates to direct oxacyclization.[44] For example, HppE can directly engage the hydroxyl group of its Pn substrate with the Fe cofactor, thus providing a plausible means of directing electron flow during radical based oxacyclization.[45] In contrast, the Fe/2OG enzymes CAS and HygX are not observed to directly bind their substrates as Fe ligands.[39,44] For this reason, the events that follow ferryl generation by these enzymes, and how rebound is suppressed, remains an intriguing avenue of inquiry.

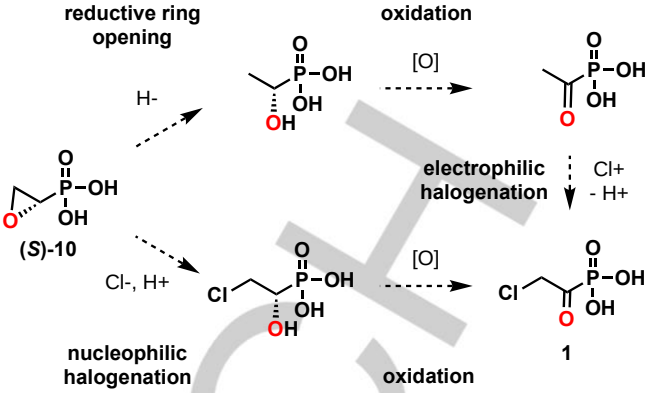


**Scheme 3.** Proposed role of the epoxide (*S*)-**10** in the biosynthesis of **1**.

## Conclusion

Our study implicates an epoxide intermediate in biosynthesis of **1** and points to a biosynthetic solution to forming the chloroacetyl group of this molecule from known Pn biosynthetic building blocks. The proposed biosynthesis of **1** involves C-P bond formation by the phosphoenolpyruvate mutase FfnA, decarboxylation by the phosphonopyruvate decarboxylase FfnB, aldehyde reduction by the NADH dependent aldo/keto reductase FfnC, then intramolecular cyclization of the resulting alcohol **8** by the Fe/2OG dependent oxacyclase FfnD to form the epoxide (*S*)-**10**. Although the reaction sequence to form the alcohol **8** is conserved in several Pn natural product pathways, including the enzymes that mediate these steps,[1] FfnC is shown in this study to be a new example of a phosphonoacetaldehyde reductase in terms of sequence and reactivity. The epoxide (*S*)-**10** formed by FfnD suggests two possible paths to forming the chloroacetyl moiety of **1**: one involving nucleophilic ring opening of the epoxide with chloride followed by oxidation of the C1 hydroxyl; the second involving reductive ring opening of the epoxide, followed by oxidation of the C1 hydroxyl and electrophilic chlorination at C2 (**Scheme 3**). FfnD is additionally significant as a model enzyme for understanding how Fe/2OG oxygenases can catalyze reactions other than substrate hydroxylation.[38,46] Due to the simplicity of the FfnD substrate, and the direct, rate limiting nature of the oxacyclization reaction catalyzed by this enzyme, the FfnD reaction provides an excellent opportunity to study how this class of enzyme can suppress oxygen rebound in favour of alternative chemistry.

## Experimental Section

**General.** All reagents were purchased from Sigma-Aldrich Canada or BioShop Canada, Inc., unless otherwise specified. $^{31}$P NMR spectra were recorded on a Bruker Avance-500 spectrometer and referenced to $H_3PO_4$ (δ = 0 ppm). Ni-NTA resin was obtained from Qiagen (Canada). Synthetic genes encoding FfnC and FfnD were obtained from Bio Basic Canada Inc. The extinction coefficients for FfnC and FfnD were calculated from their respective amino acid sequences using the ProtParam tool from ExPASy (https://web.expasy.org/protparam/). Compounds (*R*)-**14**,[47] (±)-**11**,[33] 1-[$^2H_1$]-**8**,[48] and phosphonoacetaldehyde[49] were prepared by known literature procedures. The syntheses and spectroscopic characterization of (±)-**10** and 2-[$^{18}$O]-**8** are provided in the Supporting Information.

**PepM Sequence Similarity Network Construction.** The PepM SSN was generated using the EFI Enzyme Similarity Tool[21]. The UniRef90 database for the PepM InterPro family (IPR012698) was used to perform the all-by-all BLAST analysis. An alignment score of 75 was chosen to export the SSN, which was rendered in Cytoscape. The Cytoscape file is provided in the Supporting Information.

**Production of FfnC and FfnD.** The genes encoding FfnC (XP_018236324.1) and FfnD (XP_018236329.1) were synthesized and codon optimized for expression in *E. coli*. The genes were cloned into pET28a using the *Nde*I/*Hind*III restriction sites for *ffnC* and the *Nde*I/*Xho*I restriction sites for *ffnD*, thereby encoding *N*-terminal hexa-histidine tags in the gene products. The coding sequences of the genes are given in the Supporting Information. For protein expression, the plasmids were transformed into *E. coli* BL21(DE3) cells and grown overnight at 37 °C on LB-agar supplemented with 50 µg/mL kanamycin. A single colony was used to inoculate 50 mL of LB medium with 50 µg/mL kanamycin, which was then incubated in an air shaker overnight at 37 °C and 180 rpm. From this starter culture 10 mL was transferred to 1 L of LB containing 50 µg/mL kanamycin, which was then incubated at 37 °C and 180 rpm until the culture reached an $OD_{600}$ value of 0.6. The culture was incubated on ice for 30 min followed by addition of isopropyl β-D-1-thiogalactopyranoside (IPTG) to a final concentration of 0.5 mM. The culture was then incubated at 20 °C, 180 rpm, for 18 h. The cells were subsequently harvested by centrifugation at 5,000 × *g* for 15 min. The cell pellet was flash-frozen in liquid nitrogen and stored at –30 °C until purification. For protein purification, the cell pellet was thawed on ice and suspended in buffer A (20 mM Tris-HCl, pH 7.5, 300 mM NaCl), lysed with 5 passages through an EmulsiFlex-C5 cell homogenizer (Avestin, Canada) at 15,000 psi, then centrifuged at 28,000 × *g* for 30 min at 4 °C. The clarified cell lysate was filtered through a 0.45 µm filter (Pall Corporation, California) then applied onto a 5 mL Ni-NTA Sepharose column pre-equilibrated with buffer A. The column was connected to an AKTA FPLC system then washed with 10 column volumes of buffer A at 5 mL/min, followed by a linear gradient from 4 to 100% buffer B (20 mM Tris-Cl, pH 7.5, 300 mM NaCl, 500 mM imidazole) over 10 column volumes. Pure protein fractions as identified by SDS-PAGE were combined, concentrated, and buffer exchanged into storage buffer (25 mM Tris-Cl pH 7.5, 150 mM KCl, 10% (v/v) glycerol) by ultrafiltration (Amicon, 10 kDa molecular weight cut off). Enzyme concentrations were determined by absorbance at 280 nm using the extinction coefficients $\varepsilon_{280}$ = 63,620 $M^{-1}$•$cm^{-1}$ for FfnC and 72,560 $M^{-1}$•$cm^{-1}$ for FfnD.

**Enzyme Assays.** The FfnC reaction was performed in 50 mM HEPES pH 7.25 with 20 µM FfnC, 2 mM **7**, NADH or NAD+ (1 or 10 mM), and 10 % glycerol in a total volume of 600 µL. The reaction mixture was incubated at 25 °C for 18 h then analyzed by $^{31}$P NMR spectroscopy. The FfnD reaction was performed in 50 mM HEPES pH 7.5 supplemented with 1 mg/ml bovine serum albumin (BSA) and contained 20 µM of FfnD, 2 mM of Pn substrate, 5 mM 2OG, 1 mM of ascorbic acid, 1 mM of ammonium iron (II) sulphate, and 20 mM NaCl in a total reaction volume of 600 µL. The reaction was initiated by adding 6 µL of a 100 mM stock of ammonium iron (II) sulphate (prepared in 1 mM HCl) followed by the enzyme. The reaction was incubated at 30 °C for 18 h.

**Stereochemical analysis FfnD reaction products**. The stereochemical configuration of FfnD produced epoxyethylphosphonic acid **10** (**Figure S6A**) was determined by treating the reaction mixture with 14% (v/v) ammonium hydroxide. The mixture, 2 mL, was capped and stirred at room temperature for 3 days. The reaction mixture was then stirred uncapped overnight to aid in ammonia evaporation. Next, HEPES buffer (to 50 mM final concentration) was added to the mixture and adjusted to pH 7 with a few drops of HCl using pH indicator strip for a total reaction volume of 2 mL. An aliquot of this mixture (600 µL) was used for $^{31}$P-NMR spectroscopic analysis as described below (**Figure S6B**). To confirm the identity of the aminolysis product, synthetic (*R*)-2-amino-1-hydroxyethylphosphonic acid (*R*)-**12** was added to this NMR sample (**Figure S6C**). To a second aliquot of the aminolysis mixture (480 µL) was added 12 µL of 50 mM ascorbate, 12 µL of 1 M NaCl, 6 µL of 100 mg/mL BSA, 6 µL of 100 mM ammonium iron (II) sulphate and 83 µL of *Gm*Phnz1 to afford final concentrations of 1 mM ascorbate, 20 mM NaCl, 1 mg/mL BSA, 1 mM ammonium iron (II) sulphate and 50 µM *Gm*Phnz1, in a final reaction volume of 600 µL. The reaction was incubated at 30°C for 18 hrs before $^{31}$P-NMR spectroscopic analysis (**Figure S6D**). To ensure that *Gm*PhnZ1 is active under these conditions, synthetic (*R*)-**12** was added to an identical reaction mixture as described for Figure S5D and reacted for 30°C for 18 hrs before $^{31}$P-NMR spectroscopic analysis (**Figure S6E**). The stereochemistry of 1-hydroxyethylphosphonic **14** produced by FfnD (**Figure S8A**) was determined by treatment with *Gm*PhnZ1 using the reaction conditions above (**Figure S8B**). A control reaction with *Gm*PhnZ1 using synthetic (*R*)-**14** was performed under the same conditions (**Figures S8C and D**).

**$^{31}$P NMR spectroscopic analysis of enzyme reactions.** Before $^{31}$P NMR spectroscopic analysis enzyme reactions were mixed with Chelex® 100 (Na+ form) at 30 mg resin per 600 µL reaction volume and incubated with shaking for 20 min at room temperature. The resin was removed by centrifugation (13,000 rpm for 5 min) and the supernatant was mixed with $D_2O$ [10% (v/v) final]. {$^1$H} $^{31}$P NMR spectra were recorded on a 500 MHz Bruker Avance-500 spectrometer (256 scans, 202 MHz, spectral window of -252 to 151 ppm). For $^1$H-$^{31}$P coupled NMR spectroscopic analysis, 800 scans were collected.

**Reaction of FfnD with ethylphosphonic acid and $^{18}O_2$** The FfnD reaction was performed in 50 mM HEPES pH 7.5 and contained 50 µM of FfnD, 12 mM of ethylphosphonic acid, 5 mM 2OG, 1 mM of ascorbic acid, 1 mM of ammonium iron (II) sulphate, and 20 mM NaCl in a total reaction volume of 1 mL. All reagents except for the enzyme were added to a round-bottom flask capped with a rubber septum and stirred under a gentle flow of $N_2$ gas for 1 hr to displace $^{16}O_2$. FfnD was then added via syringe, followed by approximately 500 mL of $^{18}O_2$ (Sigma Aldrich). The latter was gently introduced into the reaction flask directly from the $^{18}O_2$ cylinder via a needle and a short length of tubing and captured with a balloon attached to the flask (via a needle) to maintain positive pressure. The reaction was incubated at 21°C for 18 h, then analyzed by $^{31}$P-NMR spectroscopy to confirm the formation of 1-hydroxyethylphosphonic acid. The sample was then analyzed by high resolution MS as described in the Supporting Information.

## Acknowledgements

D.L.Z. is grateful to the Natural Sciences and Engineering Research Council (NSERC) of Canada for financial support (03695-2016). K.P. thanks the Austrian Science Fund (FWF) for support (P27987-N28).

**Keywords:** biosynthesis • metalloenzymes • iron • C-H activation • oxidation

[1] G. P. Horsman, D. L. Zechel, *Chem. Rev.* **2017**, *117*, 5704–5783.
[2] C. Zhou, X. Luo, N. Chen, L. Zhang, J. Gao, *J. Agric. Food Chem.* **2020**, *68*, 3344–3353.
[3] X. Yu, J. R. Doroghazi, S. C. Janga, J. K. Zhang, B. Circello, B. M. Griffin, D. P. Labeda, W. W. Metcalf, *Proc. Natl. Acad. Sci. U.S.A.* **2013**, *110*, 20759–20764.
[4] J. A. Blodgett, J. K. Zhang, X. Yu, W. W. Metcalf, *J. Antibiot.* **2016**, *69*, 15–25.
[5] K.-S. Ju, J. R. Doroghazi, W. W. Metcalf, *J. Ind. Microbiol. Biotechnol.* **2014**, *41*, 345–356.
[6] K.-S. Ju, J. Gao, J. R. Doroghazi, K.-K. A. Wang, C. J. Thibodeaux, S. Li, E. Metzger, J. Fudala, J. Su, J. K. Zhang, et al., *Proc. Natl. Acad. Sci. U.S.A.* **2015**, *112*, 12175–12180.

[7] K. Rice, K. Batul, J. Whiteside, J. Kelso, M. Papinski, E. Schmidt, A. Pratasouskaya, D. Wang, R. Sullivan, C. Bartlett, et al., *Nat. Comms.* **2019**, *10*, 3698–12.
[8] A. K. White, W. W. Metcalf, *Annu. Rev. Microbiol.* **2007**, *61*, 379–400.
[9] J. W. McGrath, J. P. Chin, J. P. Quinn, *Nat. Rev. Micro.* **2013**, *11*, 412–419.
[10] S. S. Kamat, F. M. Raushel, *Curr. Opin. Chem. Biol.* **2013**, *17*, 589–596.
[11] J. P. Chin, J. W. McGrath, J. P. Quinn, *Curr. Opin. Chem. Biol.* **2016**, *31*, 50–57.
[12] J. Villarreal-Chiu, J. Quinn, *Front. Microbiol.* **2012**, *3*, article 19.
[13] W. W. Metcalf, B. M. Griffin, R. M. Cicchillo, J. Gao, S. C. Janga, H. A. Cooke, B. T. Circello, B. S. Evans, W. Martens-Habbena, D. A. Stahl, et al., *Science* **2012**, *337*, 1104–1107.
[14] D. J. Repeta, S. Ferrón, O. A. Sosa, C. G. Johnson, L. D. Repeta, M. Acker, E. F. DeLong, D. M. Karl, *Nature Geosci.* **2016**, *9*, 884–887.
[15] D. M. Karl, *Nature* **2000**, *406*, 31–33.
[16] S. C. Peck, W. A. van der Donk, *Curr. Opin. Chem. Biol.* **2013**, *17*, 1–9.
[17] H. Kim, J. Chin, H. Choi, K. Baek, T.-G. Lee, S. E. Park, W. Wang, D. Hahn, I. Yang, J. Lee, et al., *Org. Lett.* **2013**, *15*, 5614–5614.
[18] M. Takeuchi, M. Nakajima, T. Ogita, M. Inukai, K. Kodama, K. Furuya, H. Nagaki, T. Haneishi, *J. Antibiot.* **1989**, *42*, 198–205.
[19] C. M. Kayrouz, Y. Zhang, T. M. Pham, K.-S. Ju, *ACS Chem. Biol.* **2020**, *15*, 1921–1929.
[20] Vinas Meneses, M. de L. A., Biosynthesis and Biological Function of Phosphonates in *Fusarium* spp., Ph.D. thesis, Georg-August-University: Gottingen, Germany, **2018**.
[21] J. A. Gerlt, J. T. Bouvier, D. B. Davidson, H. J. Imker, B. Sadkhin, D. R. Slater, K. L. Whalen, *BBA - Proteins and Proteomics* **2015**, *1854*, 1019–1037.
[22] J. Lin, M. Nishiyama, T. Kuzuyama, *J. Antibiot.* **2015**, *68*, 357–359.
[23] S. C. Peck, S. Y. Kim, B. S. Evans, W. A. van der Donk, *Med. Chem. Commun.* **2012**, *3*, 967–5.
[24] Z. Shao, J. A. V. Blodgett, B. T. Circello, A. C. Eliot, R. Woodyer, G. Li, W. A. van der Donk, W. W. Metcalf, H. Zhao, *J. Biol. Chem.* **2008**, *283*, 23161–23168.
[25] X. Zhu, A. J. Lapthorn, E. M. Ellis, *Biochemistry* **2006**, *45*, 1562–1570.
[26] E. Kozma, E. Brown, E. M. Ellis, A. J. Lapthorn, *J. Biol. Chem.* **2002**, *277*, 16285–16293.
[27] V. Agarwal, S. C. Peck, J.-H. Chen, S. A. Borisova, J. R. Chekan, W. A. van der Donk, S. K. Nair, *Chem. Biol.* **2014**, *21*, 125–135.
[28] M. A. DeSieno, W. A. van der Donk, H. Zhao, *Chem. Commun.* **2011**, *47*, 10025–10027.
[29] B. T. Circello, A. C. Eliot, J.-H. Lee, W. A. van der Donk, W. W. Metcalf, *Chem. Biol.* **2010**, *17*, 402–411.
[30] J. W. McGrath, F. Hammerschmidt, W. Preusser, J. P. Quinn, A. Schweifer, *Org. Biomol. Chem.* **2009**, *7*, 1944–1953.
[31] R. D. Woodyer, Z. Shao, P. M. Thomas, N. L. Kelleher, J. A. V. Blodgett, W. W. Metcalf, W. A. van der Donk, H. Zhao, *Chem. Biol.* **2006**, *13*, 1171–1182.
[32] A. Schweifer, F. Hammerschmidt, *Bioorg. Med. Chem. Lett.* **2008**, *18*, 3056-3059.
[33] S. R. Gama, M. Vogt, T. Kalina, K. Hupp, F. Hammerschmidt, K. Pallitsch, D. L. Zechel, *ACS Chem. Biol.* **2019**, *14*, 735–741.
[34] J. Pan, E. S. Wenger, M. L. Matthews, C. J. Pollock, M. Bhardwaj, A. J. Kim, B. D. Allen, R. B. Grossman, C. Krebs, J. M. Bollinger Jr., *J. Am. Chem. Soc.* **2019**, *141*, 15153–15165.
[35] M. S. Seo, J.-H. In, S. O. Kim, N. Y. Oh, J. Hong, J. Kim, L. Que, W. Nam, *Angew. Chem. Int. Ed.* **2004**, *43*, 2417–2420.
[36] M. Puri, A. Company, G. Sabenya, M. Costas, L. Que, *Inorg. Chem.* **2016**, *55*, 5818–5827.
[37] G. W. Cooper, W. M. Onwo, J. R. Cronin, *Geochim. Cosmochim. Acta* **1992**, *56*, 4109–4115.
[38] C. Q. Herr, R. P. Hausinger, *Trends Biochem. Sci.* **2018**, *43*, 517–532.
[39] S. Martinez, R. P. Hausinger, *J. Biol. Chem.* **2015**, *290*, 20702–20711.
[40] K. M. McCulloch, E. K. McCranie, J. A. Smith, M. Sarwar, J. L. Mathieu, B. L. Gitschlag, Y. Du, B. O. Bachmann, T. M. Iverson, *Proc. Natl. Acad. Sci. USA* **2015**, *112*, 11547–11552.
[41] C. Wang, W.-C. Chang, Y. Guo, H. Huang, S. C. Peck, M. E. Pandelia, G.-M. Lin, H.-W. Liu, C. Krebs, J. M. Bollinger Jr., *Science* **2013**, *342*, 991–995.
[42] B. Wang, J. Lu, K. D. Dubey, G. Dong, W. Lai, S. Shaik, *J. Am. Chem. Soc.* **2016**, *138*, 8489–8496.
[43] S. Zhou, J. Pan, K. M. Davis, I. Schaperdoth, B. Wang, A. K. Boal, C. Krebs, J. M. Bollinger Jr., *J. Am. Chem. Soc.* **2019**, *141*, 20397–20406.
[44] A. K. Boal, J. M. Bollinger Jr, W.-C. Chang, *Proc. Natl. Acad. Sci. U.S.A.* **2015**, 201514689.
[45] L. J. Higgins, F. Yan, P. Liu, H.-W. Liu, C. L. Drennan, *Nature* **2005**, *437*, 838–844.
[46] S.-S. Gao, N. Naowarojna, R. Cheng, X. Liu, P. Liu, *Nat. Prod. Rep.* **2018**, *35*, 792–837.
[47] L. M. van Staalduinen, F. R. McSorley, K. Schiessl, J. Séguin, P. B. Wyatt, F. Hammerschmidt, D. L. Zechel, Z. Jia, *Proc. Natl. Acad. Sci. U.S.A.* **2014**, *111*, 5171–5176.
[48] F. Hammerschmidt, H. Kählig, *J. Org. Chem.* **1991**, *56*, 2364–2370.
[49] K. Pallitsch, M. P. Rogers, F. H. Andrews, F. Hammerschmidt, M. J. McLeish, *Bioorg. Med. Chem. Lett.* **2017**, *25*, 4368–4374.

10.1002/cbic.202100352





## Entry for the Table of Contents

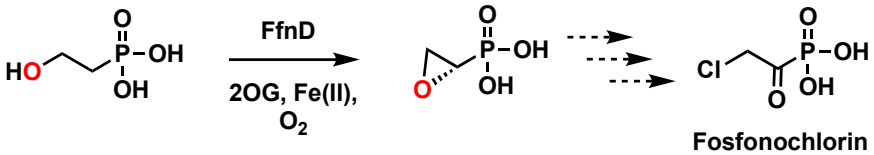


**Fosfonochlorin**

Early steps in the biosynthesis of the organophosphonate Fosfonochlorin are revealed, including a rare example of oxidative cyclization of an alcohol to form an epoxide.